Specific heat in hadronic matter and in quark-gluon matter

Ben-Hao Sa,[1,2,3,4,*] Xiao-Mei Li,[1] Shou-Yang Hu,[1] Shou-Ping Li,[1] Jing Feng,[1] and Dai-Mei Zhou[2]

[1]*China Institute of Atomic Energy, P. O. Box 275 (18), Beijing 102413, People's Republic of China*

[2]*Institute of Particle Physics, Huazhong Normal University, Wuhan 430079, People's Republic of China*

[3]*CCAST (World Laboratory), P. O. Box 8730 Beijing 100080, People's Republic of China*

[4]*Institute of Theoretical Physics, Academy Sciences, Beijing 100080, People's Republic of China*

(Received 18 May 2006; revised manuscript received 9 March 2007; published 25 May 2007)

A parton and hadron cascade model, PACIAE, is applied to follow the particle transport in partonic and the hadronic stages in 0–5% most central Au+Au collisions at energies from SPS to RHIC. We have determined the specific heat of hadron matter ($\pi^+ + \pi^-$) in the hadronic final state and the specific heat of quark-gluon matter ($u + d + g$) in the partonic initial state in Au+Au collisions as a function of the reaction energy (excitation function). It turns out that the quark-gluon matter (QGM) specific heat is hard to survive the hadronization and there is not a peak structure in the specific heat excitation functions in studied energy region.

DOI: 10.1103/PhysRevC.75.054912 PACS number(s): 24.10.Lx, 24.85.+p, 25.75.Dw

I. INTRODUCTION

The statistical model has been very successful in describing the heavy ion collision both at the intermediate energy [1–4] and the relativistic energy [5–9]. One of the most important thermodynamic variables is the heat capacity because it is a measure of the temperature (energy) fluctuation and its singularity behavior is relevant to the phase transition.

It was first reported in Ref. [1] that the peak structure in the heat capacity as a function of temperature characterizes the phase transition in disassembly of the hot nucleus (fireball) formed in the intermediate energy heavy ion collisions. This observation was further confirmed as an evidence of the liquid-gas phase transition in heavy ion collisions at intermediate energies [10–12].

In the field of relativistic heavy ion collisions a similar study was first proposed in Refs. [13,14]. A lot of investigations were then stimulated [15–23]. Although most methods used to extract the heat capacity are all based on the statistical physics [24], the resulting values are very different from each other. The specific heat of charged pions extracted from the experimental charged pion transverse momentum distribution in Pb+Pb collisions at 158A GeV [25] is 60±100 (if the average temperature $\langle T \rangle$ is 180 MeV) [16]. While a π^+ specific heat of 1.66 was extracted from the theoretical π^+ transverse mass distribution in central Pb+Pb collisions at 158A GeV [18]. A specific heat of 13.2 was found for pions in Ref. [22]. On the other hand, the specific heat of quantum chromodynamics (QCD) matter (quark-gluon-matter, QGM) was studied using the thermodynamic potential of perturbative QCD (pQCD) [17] and found that the specific heat of QGM is larger than the specific heat of an ideal gas of ∼30 (if the running coupling constant $\alpha_s = 0.65$ and the ratio of temperature to chemical potential is within $0.012 < T/\mu < 0.07$). However, in Ref. [20] it was reported that the specific heat of QGM is lower than the ideal gas (∼21, if $T/T_c = 2$ and T_c here is the critical temperature) in a pure gauge theory.

The present status in the study of specific heat is so unclear that a further study is required. In this paper we study the QGM and hadron matter (HM) heat capacities using a uniform method of a dynamical simulation followed by the statistical model. In order to explore the way of using experimental hadronic event-by-event transverse momentum distributions to measure the hadron specific heat [21], the high energy nucleus-nucleus collisions are our objective. The partons ($u + d + g$) at the initial partonic stage and the charged pions ($\pi^+ + \pi^-$) at the hadronic final stage in Au+Au collisions are regarded, respectively, as the representative of the QGM and the HM scenarios. Our goal is to study the influence of the QGM specific heat at the initial partonic state on the HM specific heat at the final hadronic state in 0–5% most central Au+Au collisions at energies from SPS to RHIC and to explore the evidence for quark-gluon plasma (QGP) phase transition. In the dynamical simulation a parton and hadron cascade model, PACIAE [26,27], is applied to follow the particle transport (first for partons and then hadrons) in Au+Au collisions. Once the HM and QGM transverse momentum distributions are calculated event-by-event, the temperature fluctuation (distribution) is extracted by fitting the transverse momentum distribution to an exponential distribution. Finally, the HM and QGM heat capacities are calculated according to the assumption in statistical physics that the temperature fluctuation should be a Gaussian distribution [24]. It turns out that there is no peak structure in the QGM and HM specific heat excitation functions in the studied energy region. However, it is hard for the QGM specific heat to survive the hadronization and to influence the HM specific heat.

II. MODEL

We first introduce the PACIAE model briefly for self-consistency. A simplified version of the PACIAE model is given in [26] and a detailed description has been published in [27]. The PACIAE model is composed of four parts: the parton initialization, the parton evolution, the hadronization, and the hadron evolution.

*Corresponding author: sabh@ciae.ac.cn

In the first part, a nucleus-nucleus collision is decomposed into nucleon-nucleon collisions. A nucleon in the colliding nucleus is randomly distributed in spatial coordinate space according to a Woods-Saxon distribution (r) and the 4π uniform distribution (θ and ϕ) and it is given the beam momentum (the Fermi motion is neglected). A distance of closest approach and the corresponding collision time are calculated for each nucleon-nucleon (NN) collision pair along their straight line trajectories under the requirement that the above distance must be less than or equal to $\sqrt{\sigma_{\rm tot}/\pi}$. Here $\sigma_{\rm tot}$ refers to the total cross section of NN collision assumed to be 45 mb. The particle list and the NN collision (time) list are constructed. A NN collision with smallest collision time is selected and decomposed into parton-parton collisions. The hard parton-parton collision is modeled by the lowest Leading-Order (LO) pQCD parton-parton interaction [28] modified by the parton distribution function in a nucleon and the soft parton-parton interaction is considered empirically [29]. Both interactions are performed by the PYTHIA model [29] where the string fragmentation is switched off. Thus the produced particles in a NN collision are the quark pairs, diquark pairs, and the gluons. The diquark (anti-diquark) splits into quarks (antiquarks) randomly. The produced partons, similar to the nucleons, propagate along a straight line trajectory in a time interval equal to the difference between last collision time and the current collision time. After a NN collision both the particle list and the NN collision list are updated. The next NN collision is selected from the updated NN collision list and the processes above are repeated until the NN collision list is empty. Therefore, the consequence of a nucleus-nucleus collision is a configuration of quarks (q), antiquarks ($\bar{q}$), and gluons (g), besides the spectator nucleons and the beam remnants [29].

The next step is the parton evolution including parton-parton scattering. Here we use a leading order (LO) pQCD differential cross section [28] regularized by the color screen mass to describe the $2\to2$ scattering processes. The differential cross section of a subprocess $ij \to kl$ reads

$$\frac{d\sigma_{ij\to kl}}{d\hat{t}} = \frac{\pi\alpha_s^2}{\hat{s}} \sum_{ij\to kl}, \tag{1}$$

where, for the subprocess $q_1q_2 \to q_1q_2$ for instance, the $\sum_{ij\to kl}$ is just

$$\sum_{q_1q_2\to q_1q_2} = \frac{4}{9}\frac{\hat{s}^2+\hat{u}^2}{(\hat{t}-\mu^2)^2}. \tag{2}$$

In the above equations the $\hat{s}, \hat{t}$, and $\hat{u}$ are the Mandelstam variables, α_s is the running coupling constant, and μ is the color screening mass. The total cross section of the parton collision $i + j$ can be obtained as

$$\sigma_{ij}(\hat{s}) = \sum_{k,l} \int_{-\hat{s}}^{0} d\hat{t} \frac{d\sigma_{ij\to kl}}{d\hat{t}}. \tag{3}$$

Thus the parton evolution can be simulated by including differential and total cross sections into a Monte Carlo calculation.

As of now, only $2\leftrightarrow2$ processes are considered. Among them there are six elastic and three inelastic channels [28]. However the parton shower [30,31] is taken into account in terms of partonic final state QCD radiation, as an option.

In the hadronization we first assume that the partons begin to hadronize when the interactions among them have ceased (freeze-out). They can hadronize by either the fragmentation model [32,33] or the coalescence model [34,35]. The fragmentation models we have used here are the independent fragmentation (IF) model (i.e., the Field-Feynman model) [32] and the Lund string fragmentation model (LSF) [33]. The program built in [29] is employed for the implementation of the fragmentation model, however we do write a program ourselves for the coalescence model. The ingredients of our coalescence model are briefly summarized as follows:

(i) The Field-Feynman parton generation mechanism [32] is applied to deexcite the energetic parton and thus to increase the parton multiplicity. This deexcitation of an energetic parton plays a similar role as the multiple fragmentation of a string in the Lund model [33].
(ii) The gluons are forcibly split into $q\bar{q}$ pair randomly.
(iii) There is a hadron table composed of mesons and baryons in the program of coalescence model. The pseudoscalar and vector mesons made of u, d, s, and c quarks, the B^+, B^0, B^{*0}, and the Υ are involved for the moment. As for the baryon, the SU(4) multiplets of baryons made of u, d, s, and c quarks (except those with double c quarks) and the Λ_b^0 are considered.
(iv) Two partons can coalesce into a meson and three partons into a baryon (antibaryon) according to both the flavor, momentum, and spatial coordinates of partons and the valence quark structure of hadron.
(v) When the coalescing partons can form either a pseudoscalar meson or a vector meson (e.g., $u\bar{d}$ can form either a π^+ or a ρ^+) a principle of less discrepancy between the invariant mass of coalescing partons and the mass of coalesced hadron is invoked to select one from them. In case of baryon the same principle is invoked to select one baryon from both of the $\frac{1}{2}^+$ and the $\frac{3}{2}^+$ baryons (e. g. both p and the Δ^+ are composed of uud).
(vi) Three momentum conservation is required.
(vii) There is a phase space requirement

$$\frac{16\pi^2}{9}\Delta r^3 \Delta p^3 = \frac{h^3}{d}, \tag{4}$$

where h^3/d is the volume occupied by a single hadron in the phase space, $d = 4$ refers to the spin and parity degeneracies, Δr and Δp stand for the spatial and momentum distances between coalescing partons, respectively.

The last part of the hadron evolution (hadronic rescattering) is followed by a hadron cascade model, LUCIAE [36], which is based on the two-body collisions.

It should be mentioned here that in the above partonic initialization process, a NN collision is ended at a partonic state where the leading nucleon is very rare. Thus a nucleon suffers only one NN collision most probably, the consequent

number of the participant nucleons ($\langle N_{\rm part}\rangle$) and the binary NN collisions ($\langle N_{\rm bin}\rangle$) may not be large enough. In order to overcome this shortcoming and to have the coherence among the four parts of the model, the simulation can be performed as follows: For each NN collision selected from the NN collision list the PYTHIA model [29] with string fragmentation switched off is applied to have a parton initial state. That is directly followed by the parton scattering, the hadronization, the upgrade of particle list, and the upgrade of NN collision list (hadronic rescattering is involved here). Such kind of simulation is referred to as the coherent version in order to distinguish with the default one.

The heat capacity, C_v, is the quantity of heat needed to raise the temperature of a system by one unit of temperature (one GeV, for instance), it reads [24]

$$C_v = T\left(\frac{\partial S}{\partial T}\right)_V = \left(\frac{\partial E}{\partial T}\right)_{V,N}, \tag{5}$$

where the T, V, N, S and the E are, respectively, the temperature, volume, number of particles, entropy, and the internal energy of the system. And the specific heat, c_v, stands for the heat capacity per particle which composes the system.

Fitting the particle transverse momentum distribution measured (or calculated) in the relativistic nucleus-nucleus collision

$$P(p_t) = \frac{1}{p_t}\frac{dN}{dp_t} \tag{6}$$

to an exponential distribution

$$P_T(p_t) = A\exp\left[-\frac{p_t}{T}\right], \tag{7}$$

the temperature can be extracted event-by-event. In the above equation A is a normalization factor and T refers to the apparent temperature.

If the reaction system (fireball) is in equilibrium, the event-by-event temperature fluctuation obeys

$$P(T) \sim \exp\left[-\frac{C_v}{2}\frac{(\Delta T)^2}{\langle T\rangle^2}\right], \tag{8}$$

where $\langle T\rangle$ is the mean (equilibrium) temperature and the $\Delta T = T - \langle T\rangle$ refers to the temperature variance [24]. Comparing the above temperature distribution to the general Gaussian distribution

$$P(x) = \frac{1}{\sqrt{2\pi}\sigma}\exp\left[-\frac{1}{2}\frac{(\Delta x)^2}{\sigma^2}\right], \tag{9}$$

where $\sigma = \langle x - \langle x\rangle\rangle$ is the standard deviation, one finds the following expression for the heat capacity [24]:

$$\frac{1}{C_v} = \frac{\langle T^2\rangle - \langle T\rangle^2}{\langle T\rangle^2}. \tag{10}$$

III. CALCULATIONS AND RESULTS

In the simulations for 0–5% most central Au+Au collisions at energies from SPS to RHIC the model parameters are fixed and the IF model [32] is adopted for hadronization in the coherent version of the PACIAE model. The results from the full model simulations will be labeled by "HM via QGM" since the hadronic final state here is evolved from the partonic initial state. If the simulation is ended at the stage of partonic scattering before hadronization the result will be referred as "QGM" (QGM scenario). In addition, a third simulation for a pure hadronic scenario is performed, where the string fragmentation in PYTHIA switches on and follows directly by the hadronic rescattering, the corresponding results will be labeled by "HM". In this third simulation only the hadron transport is taken into account similarly to the HIJING [37], RQMD [38], UrQMD [39], JPCIAE [40], and AMPT without string melting [41].

As mentioned above, the charged pion pair ($\pi^+ + \pi^-$, π^0 decay is assumed) and the parton triplet ($u + d + g$) are assumed to be the representative of HM and the QGM systems, respectively. We assume further that the temperature of HM and QGM systems is determined by fitting their multiplicity weighted transverse momentum distribution

$$P(p_t)_{\rm HM} = \frac{M_{\pi^+}}{M_{\pi^+} + M_{\pi^-}}P(p_t)_{\pi^+} + \frac{M_{\pi^-}}{M_{\pi^+} + M_{\pi^-}}P(p_t)_{\pi^-} \tag{11}$$

and

$$\begin{aligned} P(p_t)_{\rm QGM} &= \frac{M_u}{M_u + M_d + M_g}P(p_t)_u \\ &+ \frac{M_d}{M_u + M_d + M_g}P(p_t)_d \\ &+ \frac{M_g}{M_u + M_d + M_g}P(p_t)_g \end{aligned} \tag{12}$$

to Eq. (7) within $p_t \leqslant 1$ event-by-event, respectively. Once the HM and QGM heat capacity are calculated by Eq. (10) their specific heat can be calculated, respectively, by the ratio of their heat capacity to the $\langle M_{\rm HM}\rangle$ and $\langle M_{\rm QGM}\rangle$, where

$$\begin{aligned} \langle M_{\rm HM}\rangle &= \frac{\langle M_{\pi^+}\rangle}{\langle M_{\pi^+}\rangle + \langle M_{\pi^-}\rangle}\langle M_{\pi^+}\rangle \\ &+ \frac{\langle M_{\pi^-}\rangle}{\langle M_{\pi^+}\rangle + \langle M_{\pi^-}\rangle}\langle M_{\pi^-}\rangle, \end{aligned} \tag{13}$$

and

$$\begin{aligned} \langle M_{\rm QGM}\rangle &= \frac{\langle M_u\rangle^2}{\langle M_u\rangle + \langle M_d\rangle + \langle M_g\rangle} + \frac{\langle M_d\rangle^2}{\langle M_u\rangle + \langle M_d\rangle + \langle M_g\rangle} \\ &+ \frac{\langle M_g\rangle^2}{\langle M_u\rangle + \langle M_d\rangle + \langle M_g\rangle}. \end{aligned} \tag{14}$$

In the above equations the capital M is the multiplicity and the $\langle\cdots\rangle$ means the average over events. We compare HM specific heat in the "HM" and the "HM via QGM" simulations to the QGM specific heat in "QGM" simulations studying the effect of the partonic initial state on the hadronic final state and exploring the evidence for QGP phase transition in Au+Au collisions.

In Fig. 1 is given the event averaged transverse momentum distribution (within $|y| \leqslant 4$) of HM (full circles) and the QGM (open circles) systems from the "HM via QGM" and "QGM"

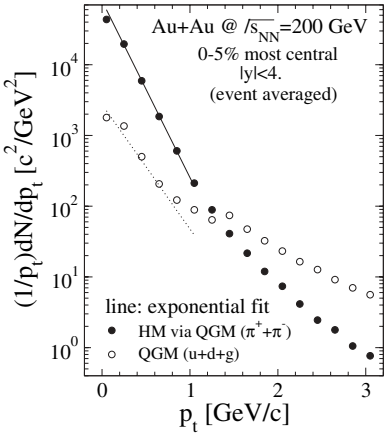

FIG. 1. The event averaged transverse momentum distribution of HM (full circles, from "HM via QGM" simulations) and QGM (open circles, from "QGM" simulations) in 0–5% most central Au+Au collisions at $\sqrt{s_{NN}} = 200$ GeV.

simulations for the 0–5% most central Au+Au collisions at $\sqrt{s_{NN}} = 200$ GeV, respectively. The solid and doted lines in this figure are the corresponding exponential fits. Similarly, the transverse momentum distribution of HM and QGM systems in a single event (impact parameter $b = 0.716$ fm) are given in Fig. 2. The common features in Figs. 1 and 2 have to be discussed:

(i) The transverse momentum distribution in QGM system is below the one in HM system in $p_t < 1.3$ GeV/c region, because the parton multiplicity in the partonic initial stage before hadronization is less than the hadron multiplicity in hadronic final state.
(ii) The slope of the QGM transverse momentum distribution is less than the HM in $p_t < 1.3$ GeV/c region, because the temperature in the partonic initial state is higher than the one in the hadronic final state.
(iii) The QGM transverse momentum distribution is much harder than the HM transverse momentum distribution in $p_t > 1.3$ GeV/c region. One have just to rely on the multiple fragmentations of the energetic quark (in IF model) and/or string (in LSF model) in order that the hadron multiplicity in the final hadronic state is larger than the parton multiplicity in the initial partonic stage by a factor of four. That means a strong increase of the system entropy during the hadronization.

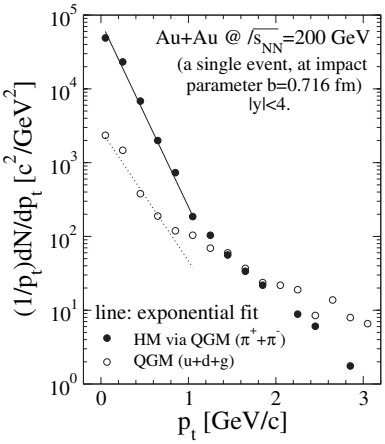

FIG. 2. The transverse momentum distribution of HM (full circles, from "HM via QGM" simulations) and QGM (open circles, from "QGM" simulations) in a single event of most central ($b = 0.716$ fm) Au+Au collision at $\sqrt{s_{NN}} = 200$ GeV.

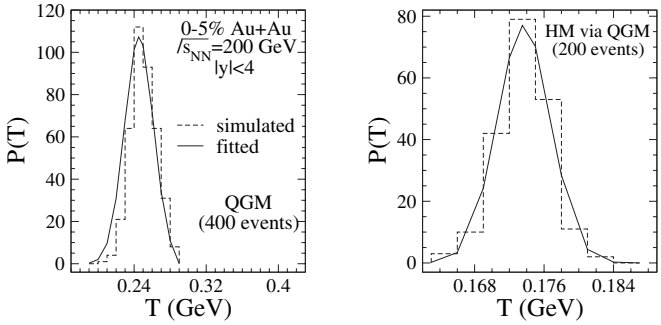

FIG. 3. The QGM temperature distribution (left panel, from "QGM" simulations) and the HM temperature distribution (right panel, from "HM via QGM" simulations) in 0–5% most central Au+Au collisions at top RHIC energy. The histogram and curve are from the simulation and fitting, respectively.

The QGM temperature distribution (left panel, from "QGM" simulations) and the HM temperature distribution (right panel, from "HM via QGM" simulations) in 0–5% most central Au+Au collisions at $\sqrt{s_{NN}} = 200$ GeV are given in Fig. 3. In this figure the dashed histograms are simulated results and the solid curves are the corresponding fit by Eq. (9), respectively. One sees in this figure that the QGM in the initial partonic stage and the HM in the final hadronic stage are reasonably to be assumed in equilibrium.

The QGM and HM temperature and specific heat excitation functions are given in the upper and lower panels in Fig. 4, respectively. In this figure the squares, circles, and the triangles are, respectively, from the "QGM", "HM via QGM", and the "HM" simulations. We see in the upper panel that either the QGM or the HM temperature increases with the increasing of reaction energy and the QGM temperature is always higher than the HM. The "HM via QGM" temperature is higher than "HM" indicating the the effect of the initial partonic state on the final hadronic state. However, one knows in lower panel that the trends of the specific heat is opposite to the temperature because the specific heat is a measure of the temperature fluctuation and the higher temperature the lower fluctuation. The "HM via QGM" specific heat excitation function is a little higher than the "HM", that can attribute to the competition between fluctuations of temperature and the multiplicity. The "HM via QGM" specific heat is close to the "HM" indicating the difficulty of QGM specific heat to survive the hadronization.

As mentioned above, our method is similar to the one used in Refs. [16,18], thus our HM specific heat of ∼1.94 in "HM" simulations for 0–5% most central Au+Au collisions at $\sqrt{s_{NN}} = 17.3$ falls in the bounds given in [16] (60±100). The difference between our result of 1.94 and 1.66 in Ref. [18] can attribute to the differences in the reaction system

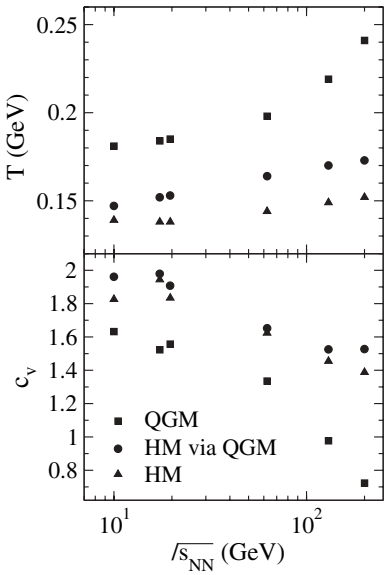

FIG. 4. The excitation function of temperature (upper panel) and specific heat (lower panel) in 0–5% most central Au+Au collisions at energies from SPS to RHIC. The squares, circles, and triangles are from "QGM", "HM via QGM", and "HM" simulations, respectively.

(Au+Au vs Pb+Pb), the dynamic simulation model, and the model parameters. However, our result is nearly a factor of 7 smaller than the result of 13.2 in a complete statistical model [22]. The differences among our QGM specific heat, the QCD matter specific heat in a pQCD thermodynamic method (∼10, if $T/\mu = 0.1$ is assumed) [17], and the QCD matter specific heat in an approximate pure gauge theory (∼15, if $T/T_c = 2$) [20] are quite big. Whether the difference between classical statistics and quantum statistics can account for such a big discrepancy has to be studied further. We suggest using RHIC single event charged pion transverse momentum distribution data to extract the charged pion specific heat exactly according to the same statistical method used here. That can rule out the bad methods for the HM system first. The corresponding work is progressing.

However, it is interesting to stress that there is not peak structure in the specific heat excitation functions in the studied energy region, unlike the results in [1,10–12] where the fix volume is better satisfied. The conditions of fixed volume and multiplicity are strong assumptions in the relativistic heavy ion collisions. Because in the relativistic nucleus-nucleus collisions (experiments or simulations) only the event averaged (mean) particle multiplicity is fixed for instance and the particle multiplicity in a single event is fluctuated around the mean multiplicity. However, the strong assumption of fixed volume and multiplicity were introduced in all the studies for heat capacity in the heavy ion collisions [15,16,18,19,21–23]. How to satisfy the above thermodynamic conditions in the experimental and/or theoretical studies of the specific heat based on statistical physics in the heavy ion collisions is really an open question. Recently it has been attempted using a method of the event selection and/or source reconstruction to deal with the connection between thermodynamic and the hadronic final state in heavy ion collisions experimentally in Refs. [42,43]. Before solving this connection properly in experiment and the theory, it is still too early to conclude whether a peak structure is there or not in the specific heat excitation functions in heavy ion collisions from the AGS and SPS to the RHIC and LHC energies.

In summary, a parton and hadron cascade model, PACIAE, is applied investigating the specific heat for both the QGM scenario in initial partonic stage ("QGM") and the HM scenario in final hadronic stage ("HM via QGM") in 0–5% most central Au+Au collisions at energies from SPS to RHIC. In addition, the HM specific heat is also simulated for a pure hadronic matter ("HM") where the hadron transport is considered only. The HM specific heat excitation function resulting from "HM via QGM" simulations is close to the one from "HM" simulations. That indicates the QGM specific heat is hard to survive the hadronization. However, there is not peak structure in the QGM and HM specific heat excitation functions in the studied energy region.

ACKNOWLEDGMENTS

The fruitful discussions with Yu-Gang Ma, Guo-Liang Ma, and Peng-Fei Zhuang and the financial support from NSFC (10475032, 10545003, and 10635020) in China are acknowledged.

[1] Ben-Hao Sa and D. H. E. Gross, Nucl. Phys. **A437**, 643 (1985).
[2] J. P. Bondorf, R. Donangelo, I. N. Mishustin, C. J. Pethick, H. Schulz, and K. Sneppen, Nucl. Phys. **A443**, 321 (1985).
[3] J. P. Bondorf, S. Botvina, A. S. Iljinov, I. N. Mishustin, and K. Sneppen, Phys. Rep. **257**, 133 (1995).
[4] D. H. E. Gross, Phys. Rep. **279**, 120 (1997).
[5] P. Braun-Munzinger and J. Stachel, Nucl. Phys. **A606**, 320 (1986).
[6] J. Cleymans, H. Oeschler, and K. Redlich, Phys. Rev. C **59**, 1663 (1999).
[7] J. Zimanyi, Nucl. Phys. **A661**, 224c (1999).
[8] Zhong-Dao Lu, A. Faessler, C. Fuchs, and E. E. Zabrodin, Phys. Rev. C **66**, 044905 (2002).
[9] F. Becattini, M. Gazdzicki, A. Keranen, J. Manninen, and R. Stock, Phys. Rev. C **69**, 024905 (2004).
[10] J. P. Bondorf, R. Donangelo, I. N. Mishustin, and H. Schulz, Nucl. Phys. **A444**, 460 (1985).
[11] S. Das Gupta and A. Z. Mekjian, Phys. Rev. C **57**, 1361 (1998).
[12] C. Das, S. Das Gupta, W. Lynch, A. Z. Mekjian, and B. Tsang, Phys. Rep. **406**, 1 (2005).
[13] L. Stodolsky, Phys. Rev. Lett. **75**, 1044 (1995).
[14] E. V. Shuryak, Phys. Lett. **B423**, 9 (1998).
[15] M. Stephanov, K. Rajagopal, and E. Shuryak, Phys. Rev. D **60**, 114028 (1999).
[16] R. Korus, St. Mrowczyński, M. Rybczyński, and Z. Wlodarczyk, Phys. Rev. C **64**, 054908 (2001).

[17] A. Ipp, A. Gerhold, and A. Rebhan, Phys. Rev. D **69**, 011901(R) (2004).
[18] Guo-Liang Ma *et al*., High Energe Phys. and Nucl. Phys. **28**, 398 (2004) (in Chinese).
[19] Yu-Gang Ma *et al*., J. Phys. G: Nucl. Part. Phys. **31**, S1179 (2005).
[20] R. V. Gavai, S. Gupta, and S. Mukherjee, Phys. Rev. D **71**, 074013 (2005).
[21] M. J. Tannenbaum, nucl-ex/0512004.
[22] A. Mekjian, Phys. Rev. C **73**, 014901 (2006).
[23] H. Heiselberg, Phys. Rep. **351**, 161 (2001).
[24] L. D. Laudau and E. M. Lifschitz, *Course of Theoretical Physics*, Vol. 5, Statistical Physics, Sect. 111 (Pergamon Press, London-Paris, 1958).
[25] H. Appelshäuser *et al*., Phys. Lett. **B459**, 679 (1999).
[26] Ben-Hao Sa and Aldo Bonasera, Phys. Rev. C **70**, 034904 (2004).
[27] Ben-Hao Sa, Dai-Mei Zhou, and Zhi-Guang Tan, J. Phys. G: Nucl. Part. Phys. **32**, 243 (2006); Dai-Mei Zhou, Xiao-Mei Li, Bao-Guo Dong, and Ben-Hao Sa, Phys. Lett. **B638**, 461 (2006).
[28] B. L. Combridge, J. Kripfgang, and J. Ranft, Phys. Lett. **B70**, 234 (1977).
[29] T. Sjöstrand, Comput. Phys. Commun. **82**, 74 (1994).
[30] M. Bengtsson and T. Sjöstrand, Nucl. Phys. **B289**, 810 (1987).
[31] B. R. Webber, Annu. Rev. Nucl. Part. Sci. **36**, 253 (1986).
[32] R. D. Field and R. P. Feynman, Phys. Rev. D **15**, 2590 (1977); Nucl. Phys. **B138**, 1 (1978); R. P. Feynman, R. D. Field, and G. C. Fox, Phys. Rev. D **18**, 3320 (1978).
[33] B. Andersson, G. Gustafson, G. Ingelman, and T. Sjöstrand, Phys. Rep. **97**, 33 (1983); B. Andersson, G. Gustafson, and B. Söderberg, Nucl. Phys. **B264**, 29 (1986).
[34] T. S. Biro, P. Levai, and J. Zimanyi, Phys. Lett. **B347**, 6 (1995).
[35] P. Csizmadia, P. Levai, S. E. Vance, T. S. Biro, M. Gyulassy, and J. Zimanyi, J. Phys. G **25**, 321 (1999).
[36] Sa Ben-Hao and Tai An, Comput. Phys. Commun. **90**, 121 (1995); Tai An and Sa Ben-Hao, *ibid*. **116**, 353 (1999).
[37] M. Gyulassy and X.-N. Wang, Comput. Phys. Commun. **83**, 307 (1994).
[38] H. Sorge, M. Berenguer, H. Stöcker, and W. Greiner, Phys. Lett. **B289**, 6 (1992).
[39] S. A. Bass *et al*., Prog. Part. Nucl. Phys. **41**, 225 (1998).
[40] Ben-Hao Sa, An Tai, Hui Wang, and Feng-He Liu, Phys. Rev. C **59**, 2728 (1999).
[41] Zi-Wei Lin, Che-Ming Ko, Bao-An Li, Bin Zhang, and S. Pal, Phys. Rev. C **72**, 064901 (2005).
[42] M. D'Agostino *et al*., Phys. Lett. **B473**, 219 (2000).
[43] M. D'Agostino *et al*., Nucl. Phys. **A749**, 55c (2005).